

Griffiths effects of the susceptible-infected-susceptible epidemic model on random power-law networks

Wesley Cota,^{1,*} Silvio C. Ferreira,^{1,†} and Géza Ódor^{2,‡}

¹*Departamento de Física, Universidade Federal de Viçosa, 36570-000, Viçosa, MG, Brazil*

²*MTA-MFA-EK Research Institute for Technical Physics and Materials Science, H-1121 Budapest, P. O. Box 49, Hungary*

(Received 16 December 2015; published 28 March 2016)

We provide numerical evidence for slow dynamics of the susceptible-infected-susceptible model evolving on finite-size random networks with power-law degree distributions. Extensive simulations were done by averaging the activity density over many realizations of networks. We investigated the effects of outliers in both highly fluctuating (natural cutoff) and nonfluctuating (hard cutoff) most connected vertices. Logarithmic and power-law decays in time were found for natural and hard cutoffs, respectively. This happens in extended regions of the control parameter space $\lambda_1 < \lambda < \lambda_2$, suggesting Griffiths effects, induced by the topological inhomogeneities. Optimal fluctuation theory considering sample-to-sample fluctuations of the pseudothresholds is presented to explain the observed slow dynamics. A quasistationary analysis shows that response functions remain bounded at λ_2 . We argue these to be signals of a smeared transition. However, in the thermodynamic limit the Griffiths effects lose their relevancy and have a conventional critical point at $\lambda_c = 0$. Since many real networks are composed by heterogeneous and weakly connected modules, the slow dynamics found in our analysis of independent and finite networks can play an important role for the deeper understanding of such systems.

DOI: [10.1103/PhysRevE.93.032322](https://doi.org/10.1103/PhysRevE.93.032322)

I. INTRODUCTION

Quenched randomness in interacting dynamical systems causes nontrivial critical behavior in nonequilibrium finite-dimensional systems [1–6]. Spatial randomness can be introduced, among other ways, in the form of dilution [7–9] or nonuniformity of the control parameters [6,10,11] or by topological heterogeneity of the connectivity structure of the interactions [3,4,12–14]. One of the most noticeable effects of quenched (or quasistatic) disorder is the onset of dynamical criticality, manifested in diverging correlation times and slow decays of the order parameter in extended regions of the parameter space, rid of fine tuning [2]. This allows a potential for explaining widespread observation of criticality, even without the assumption of self-organized mechanisms [15].

Extended criticality induced by quenched disorder is grounded on the existence of rare regions (RRs), which are large, randomly occurring patches that can linger for long times in a phase that differs from the global state of the system. Let's consider interacting dynamical systems with active and inactive (absorbing) phases and a control parameter λ such that for $\lambda > \lambda_c$ the system is globally active (supercritical) and for $\lambda < \lambda_0$ it is inactive without long lived active RRs [2]. For $\lambda_0 < \lambda < \lambda_c$, the activity in RRs lasts for very long (exponential in patch size) periods but fluctuations unavoidably end up the local activity due the finite size of the patches. Convolution of low-probability RRs and exponentially long lifetimes results in a slow dynamics with nonuniversal exponents in the interval $\lambda_0 < \lambda < \lambda_c$ called Griffiths phase (GP) [5,16].

Complex networks constitute a fundamental theoretical framework to describe substrates where many dynamical processes, as epidemics, information, and transportation take place [17,18]. Heterogeneity (disorder) is an intrinsic hallmark of complex networks manifested through several forms of centralities [19]. The degree-centrality ranks among the most basic properties and is statistically represented by the degree probability distribution $P(k)$ that a randomly selected vertex of the network has k connections [18]. Many networks observed in nature have highly heterogeneous patterns of connectivity usually described by a power-law (PL) degree distribution. These can be scale-free (SF) networks [20], characterized by heavy-tailed distribution $P(k)$ with the ratio $\langle k^2 \rangle / \langle k \rangle \gg \langle k \rangle$. Other important measure of the dynamics on networks is the eigenvector centrality [19] associated with the principal eigenvector of the adjacency matrix defined as $A_{ij} = 1$ if vertices i and j are connected and 0 otherwise.

This intrinsic disordered nature of networks calls for analogues of GP and RR phenomena. This issue has recently been investigated [3,13] and GPs have been found in the contact process (CP) [21] on finite-dimensional networks. It was conjectured that GPs are not present in models on infinite-dimensional, small-world graphs, where the average distance between vertices increases logarithmically or slower with the network size [20] as, for example, the case of random PL networks. On the other hand, at models defined on hierarchical modular structures, where the intermodule connectivity is weak, GPs were reported [4,14].

The susceptible-infected-susceptible (SIS) epidemic model [22], in which infected vertices spontaneously heal with rate 1 (fixing the time scale) and infect each of the susceptible nearest neighbors with rate λ , is a paradigmatic example of a nontrivial dynamical process on complex networks. Differing from other dynamical processes with transitions from active to inactive states, the SIS threshold is governed by the activation

*wesley.cota@ufv.br

†silviojr@ufv.br

‡odor@mfa.kfki.hu

of hubs, also called star subgraphs, and their mutual reinfection through connected paths [23–26]. As a consequence, the threshold is proved to be null in the infinite size limit for random networks with PL degree distribution $P(k) \sim k^{-\gamma}$, irrespective of the degree exponent γ [23].¹ Some interesting physical mechanisms behind the rigorous proof of Chatterjee and Durrett [23] were used by Boguñá *et al.* [25] to unveil the nature of the epidemic threshold of the SIS model. Stars are graphs with $k \gg 1$ leaves connected to a center that can themselves sustain long-term epidemic activity if $k \gg 1/\lambda^2$. In PL networks the average highest degree diverges with the network size [27], implying that more and more hubs become active stars at finite values of λ . Due to the small-world property of random PL networks, the lifetime of hubs is large enough to permit infecting each other, sustaining epidemic activity in the network [25,26].

In finite random networks, the SIS dynamics is puzzling due to the highly fluctuating size and the number of stars realized in a network sample [28–31]. Indeed, the effective finite-size epidemic threshold is finite [25,28] since $k \ll 1/\lambda^2$ for sufficiently small values of λ and stars alone cannot sustain a long-term activity. Several network realizations have just a few vertices with degree much larger than the rest of network, hereafter called outliers. Outliers can sustain localized epidemics, with different activation thresholds for very long times, producing multiple transitions [31]. Neglecting interactions among hubs, Lee *et al.* [30] predicted that the threshold for an endemic phase, in which a finite fraction of infected vertices is present, should take place at a finite value for $\gamma > 3$, where $\langle k^2 \rangle$ is finite. According to Lee *et al.* [30], the subcritical region is ruled by a GP, with an ultraslow (logarithmic) decay of activity, in odds with the rigorous results of null threshold for infinite PL networks [23]. This proposition was supported by numerical simulations on very large, but finite, random PL networks [31]. Finally, in finite PL networks, a vanishing epidemic threshold is predicted by the quenched mean-field (QMF) theory [32,33], in which the full connectivity structure of the network is included through the adjacency matrix [29]. In such models, Griffiths effects were also shown in the localized phase for $\gamma > 3$ [34]. RR effects, localization, and heavy tailed dynamics have also been shown in spreading models defined on weighted PL networks by suppressing hub infection via disassortative weight schemes [35,36], in random networks [37,38], or in aging Barabasi-Albert graphs [37].

Although localization effects were obtained in simulations on finite networks [31], the investigated systems were very large ($\sim 10^8$ vertices), suggesting that these can be observable and relevant in many unavoidably finite real networks. Aiming at a deeper understanding of the intricate behavior of epidemic spreading on finite-size networks, we investigate the dynamics of the SIS model on a large ensemble of PL networks, using extensive numerical simulations. We show that the averaging over many independent graph realizations exhibits a slow dynamics, analogous to GPs, in an interval of control parameter

$\lambda_1 < \lambda < \lambda_2$. This region is delimited by two transitions: The former is related to the activation of the most connected hub of the network, while the latter is related to a smeared phase transition [2]. Our results indicate that this region shrinks as the size of the network increases and disappears in the thermodynamic limit, implying the absence of GPs. This is in agreement with the conjecture that finite dimensionality is required for the existence of GPs [3]. Moreover, many real networks, as, for instance, brain connectomes, have a modular organization, where modules are finite, heterogeneous, and weakly connected [39]. Slow dynamics has been reported in models defined on hierarchical modular networks [4,14,40]. Therefore, performing analysis over independent, finite networks can be useful to understand these systems.

We have organized the paper as follows. The epidemic model and the simulation methods are described in Sec. II. Results for the density decay and quasistationary simulations are presented and discussed in Secs. III and V, respectively. An optimal fluctuation theory to explain the observed slow dynamics is developed in Sec. IV. Our concluding remarks are presented in Sec. VI.

II. MODELS AND METHODS

The SIS model is defined as follows. Individuals lie in the vertices of a quenched network of size N and can be in two states: infected or susceptible. An infected individual i becomes spontaneously susceptible with rate 1, while a susceptible one turns to the infected state with rate λn_i , where n_i is the number of infected nearest neighbors of i . The dynamics is simulated on networks obtained by the configuration model [19] with PL distribution $P(k) \sim k^{-\gamma}$, minimum degree k_0 , and upper cutoff k_{\max} . Different cutoffs were investigated: Free ($k_{\max} = N$, strictly and is also called natural), hard ($k_{\max} = k_0 N^{0.9/(\gamma-1)}$), and structural ($k_{\max} = \sqrt{N}$) cutoffs. The first one leads to degree distributions in which both the average and the standard deviation of the highly fluctuating natural cutoff diverge as $N^{1/(\gamma-1)}$ [31]. Conversely, the second one is engineered to render distributions without very large gaps in their tails of the degree distribution, since the factor 0.9 guarantees that $\sqrt{\langle k_{\max}^2 \rangle} - \langle k_{\max} \rangle^2 / \langle k_{\max} \rangle \rightarrow 0$ as $N \rightarrow \infty$ [31]. The structural cutoff is not fluctuating and guarantees the absence of degree correlations for $\gamma < 3$ and becomes equivalent to the absence of a cutoff for $\gamma > 3$ and $N \rightarrow \infty$ [27]. Graph edges are generated randomly, forbidding multiple and self-connections. All simulations were performed for $k_0 = 3$. Three ranges of the degree exponents were considered separately: $\gamma > 3$, for which localization is conjectured by the QMF theory [29]; $\gamma < 2.5$, where nonlocalized epidemic spreading is predicted [30,41]; and $2.5 < \gamma < 3$ strict SF regime, where localization is conjectured by the QMF theory [29,41].

The simulations were run using the modified Gillespie algorithm described in Refs. [28,31]. The number of infected vertices n and the number of edges S emanating from them are computed and constantly updated. With probability $1/(n + \lambda S)$ an infected vertex is randomly chosen and cured. With the complementary probability, $\lambda S/(n + \lambda S)$, an infected vertex j is chosen with a probability proportional to its degree.

¹Reference [23] calls the model known in the physics literature as SIS of “contact process.”

A vertex in the neighborhood of j is chosen with equal chance and, if it is susceptible, becomes infected, otherwise the simulation runs to next step. The time is incremented by $\Delta t = 1/(n + \lambda S)$ and the procedure is repeated iteratively.

We performed both standard and quasistationary (QS) analysis. In the former, the decay from a fully infected initial state was investigated. In the latter, only samples that did not visit the absorbing state are used to compute statistics and the analysis was done in the (quasi) stationary regime [42]. We used the improved QS method of Ref. [43], with parameters similar to those given in Ref. [31]. Differently from previous analysis of SIS on SF networks [25,28,31,33], we aim at the average behavior of a large number \mathcal{N} of independent realizations. In the decay analysis, 10 to 100 independent runs were performed for each network, being the largest number of runs used for smallest value of the infection rate.

III. TIME-DEPENDENT ANALYSIS

A. Free cutoff

Simulations for networks with a free cutoff are shown in Fig. 1. We observe an extremely slow logarithmic decay in an extended region of the control parameter λ . For $\gamma = 3.5$, the decay is very well fitted by

$$\rho \sim (\ln t)^{2-\gamma}. \tag{1}$$

For $\gamma = 2.7$, in the SF regime, we also see a logarithmic decay $\rho \sim (\ln t)^{-\alpha}$, with a varying exponent α that is not qualitatively well described by Eq. (1). The origin of the logarithmic decay given by Eq. (1) is related to the presence of the outliers in the network and will be analytically explained in Sec. IV using an optimal fluctuation theory.

B. Hard cutoff

The localization of the QMF theory for $\gamma > 2.5$ is concentrated around the largest hub [44]. So the role played by the hubs can be evidenced damping their number and fluctuations. Evolution of the density of infected vertices for hard cutoff of $P(k)$ is shown in Fig. 2 for $\gamma = 3.5$ and 2.7. The data indicate PL decay with nonuniversal exponents at long times for both degree exponents. Regressions fits: $\rho \sim t^{-\alpha(\lambda)}$ at $\gamma = 3.5$ resulted in α varying from 0.70 to 0.17 by increasing λ from 0.088 to 0.095. Similar range of exponents were found for $\gamma = 2.7$, varying λ from 0.030 to 0.0365.

C. Structural cutoff

We also simulated the density decay in networks with the structural cutoff $k_c = N^{1/2}$ with $\gamma < 3$ since otherwise it is equivalent to the natural one. This cutoff leads to the uncorrelated configuration model (UCM) [45], that has been used in many analyses of SIS on SF networks [25,28,30,33,41,46]. Power-law decays in time are still observed, but the extended region is reduced compared with hard cutoffs, see Fig. 3.

D. Sample-to-sample fluctuations

The origin of the slow decay is the sample-to-sample fluctuations rather than occurrence of rare regions in the same network. Figure 4 shows the decay of the density for 50 networks with all parameters fixed to values for which

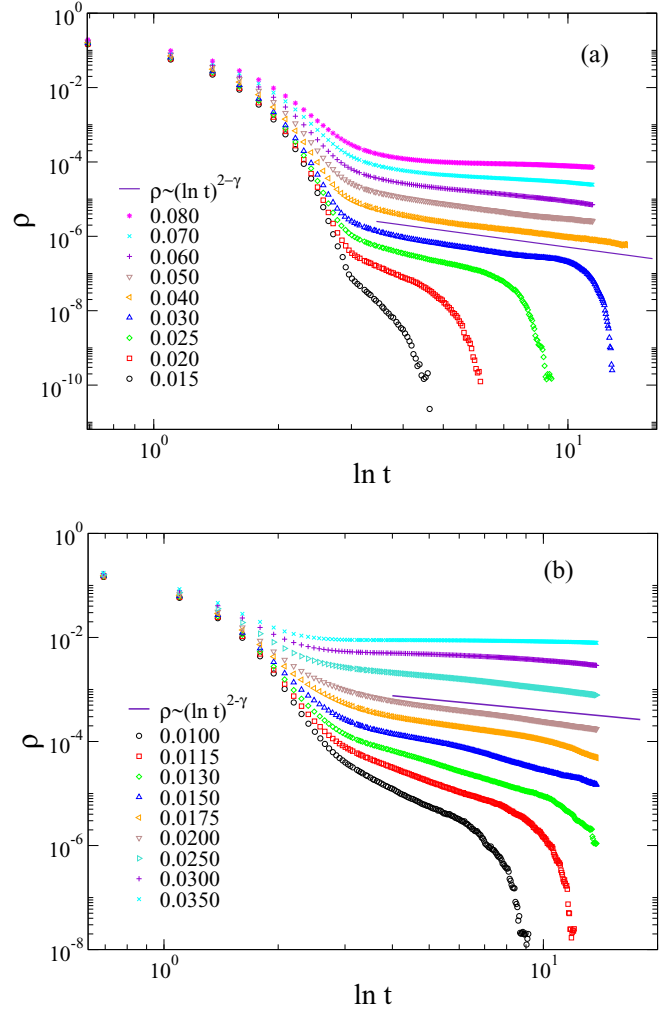


FIG. 1. Decay of density of infected vertices for networks with free upper cutoff ($k_{\max} = N$) using (a) $\gamma = 3.5$ and (b) $\gamma = 2.7$ for networks with sizes $N = 10^7$ and $N = 10^5$, respectively. The number of samples were up to $\mathcal{N} = 500$ and 4000 for $\gamma = 3.5$ and 2.7, respectively. Lines are predictions of the optimal fluctuation theory in Sec. IV. The values of λ are indicated in the legends.

slow decays are observed in the averaged curves. One can see that several curves are subcritical, while others behave supercritically, evolving to a metastable stationary density value before falling in the absorbing state. Numerically, we observe pseudothresholds and, consequently, all quantities of interest with wide distributions whose relative variance does not decrease with the network size within the region of Griffiths effects. This means that the quenched disorder is relevant within the dynamical critical region analogously to a lack of self-averaging [47], where having many finite samples is not equivalent to averaging over a single large network [18]; note that the dynamical critical region where disorder is relevant diminishes as network size increases and disappears in the thermodynamical limit, as discussed later.

There exist two main mechanisms for this large variation, the leading one depends on γ and the cutoff used. For a free cutoff, the size of the largest hubs fluctuates greatly. So the presence of outliers, creating local active domains, determines if the dynamics levels off to a quasi steady state

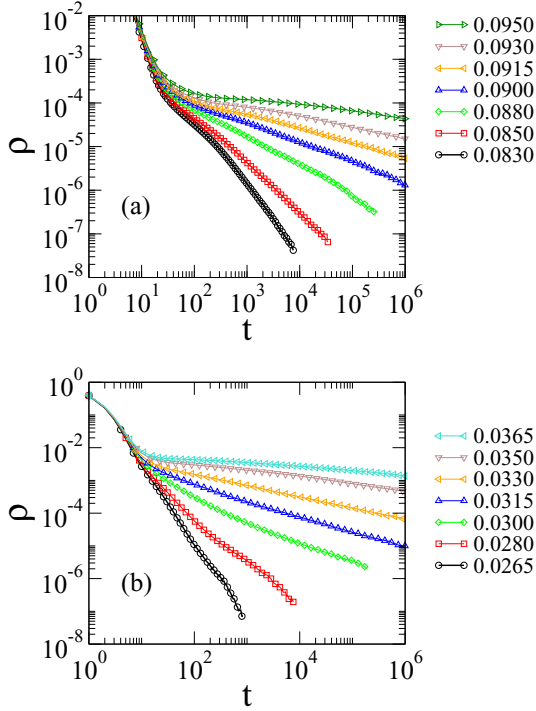


FIG. 2. Decay of density of infected vertices for (a) $\gamma = 3.5$ and (b) $\gamma = 2.7$ for networks of sizes $N = 10^7$ and 10^5 , respectively, using hard cutoff $k_c = k_0 N^{0.9/(\gamma-1)}$. The numbers of independent networks are $\mathcal{N} = 500$ and 4000 for $\gamma = 3.5$ and 2.7 , respectively. The values of λ are indicated in the legends.

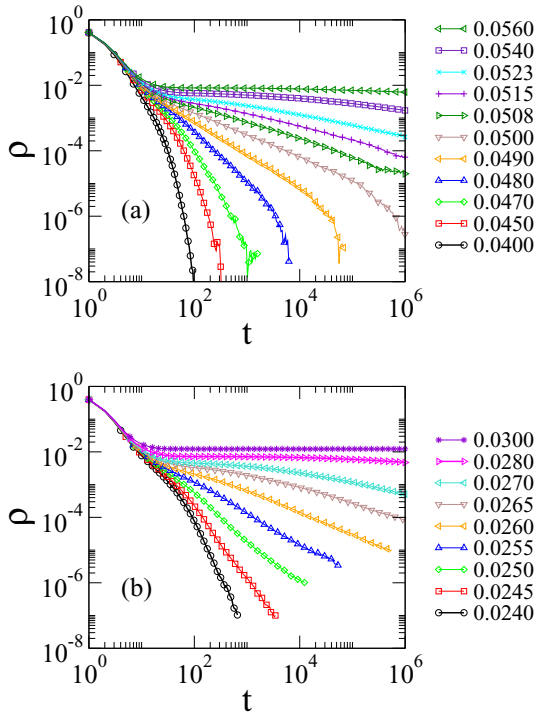


FIG. 3. Decay of density of infected vertices for (a) $\gamma = 2.7$ and (b) $\gamma = 2.3$ for networks of size $N = 10^5$ using structural cutoff $k_c = N^{1/2}$. The values of λ are indicated in the legends.

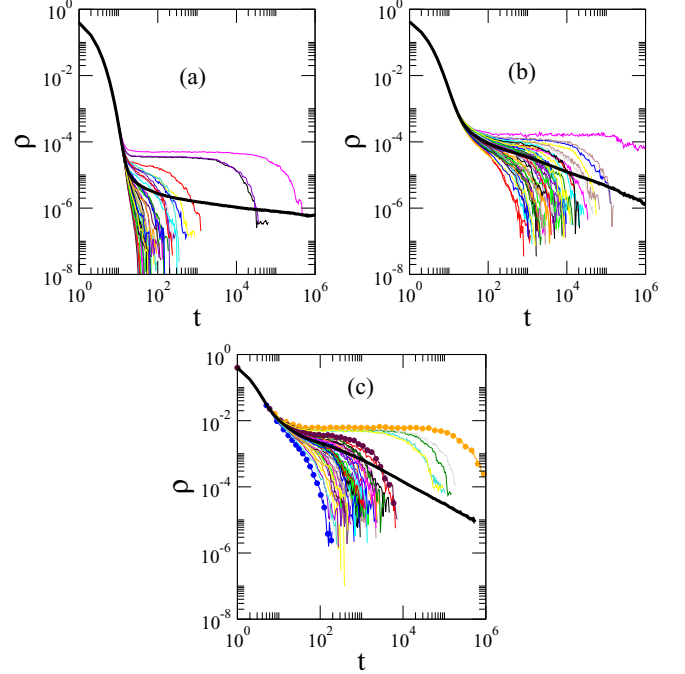


FIG. 4. Sample-to-sample fluctuation of the evolution of SIS on PL networks: (a) $\gamma = 3.5$, $N = 10^7$, free cutoff, and $\lambda = 0.04$; (b) $\gamma = 3.5$, hard cutoff $k_c = k_0 N^{0.9/(\gamma-1)}$, $N = 10^7$, and $\lambda = 0.09$; (c) $\gamma = 2.3$, structural cutoff $k_c = N^{1/2}$, $N = 10^5$, and $\lambda = 0.026$. Curves for 50 independent networks are shown. Thick lines represent the average of $\mathcal{N} = 500$ and 2000 samples for $\gamma = 3.5$ and 2.3 , respectively.

in the simulation of that sample. In the cases of hard or structural cutoffs, the tails of the degree distributions fluctuate little and the leading mechanism is the variation of the overall heterogeneity of the network, which can be measured by the average degree of the nearest neighbors of the vertices k_{nn} [48]. For the structural cutoff case this becomes $k_{nn} = \langle k^2 \rangle / \langle k \rangle$ [27], whose inverse provides a very precise estimate of the SIS epidemic threshold for $\gamma < 2.5$ [28,46]. Density decay for networks with $\gamma = 2.3$, using a structural cutoff, are shown in Fig. 4(c). Three samples highlighted with symbols possess $\langle k \rangle / \langle k^2 \rangle = 0.0270, 0.0243, \text{ and } 0.0235$, and the larger values the lower densities. These values must be compared with the infection rate $\lambda = 0.026$ used in all samples. We see that samples for which $\langle k \rangle / \langle k^2 \rangle \lesssim \lambda$ are supercritical and those where $\langle k \rangle / \langle k^2 \rangle \gtrsim \lambda$ are subcritical. An optimal fluctuation theory to explain this slow dynamics is presented in Sec. IV.

E. Finite-size analysis

The slow dynamics observed in the ensemble averages is not a genuine Griffiths singularity, since it is not triggered by the slowly decaying RRs; thus we can expect that these effects disappear in the thermodynamic limit. This conjecture is confirmed in Fig. 5, where we show the density of infected vertices against time for different sizes for a fixed infection rate $\lambda = 0.088$. We see that the dynamics is deeply subcritical, an exponential decay of activity, for $N = 10^6$. For size $N = 10^7$ a PL regime can be observed but, finally, a saturation to a constant plateau develops at $N = 10^8$. The disappearance

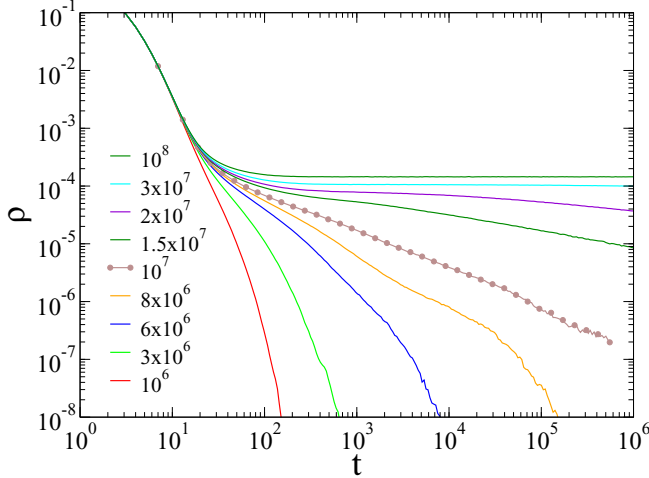


FIG. 5. Finite-size analysis of the density decay against time for networks with $\gamma = 3.5$ and hard cutoff $k_c = k_0 N^{0.9/(\gamma-1)}$ for infection rate $\lambda = 0.088$. The number of network samples is 100 for the two largest sizes and 500 for the others. The network sizes are indicated in the legends.

of the PL regimes is mainly associated with the shift of the epidemic threshold towards zero as the size increases [28,46]. The threshold drops from approximately 0.12 for $N = 10^6$ to 0.075 for $N = 10^8$. Similar finite-size effects were observed in the CP on weighted trees [35] and the same mechanism shown here is probably also present there. The CP also exhibits strong finite-size dependence of the thresholds, approaching the asymptotic value only at exceeding large networks [49,50]. Moreover, the range of λ where PLs are observed decreases as $N \rightarrow \infty$ (see also Sec. V), thus Griffiths effects disappear in the thermodynamic limit.

IV. OPTIMAL FLUCTUATION THEORY

The hypothesis drawn in Sec. III, in which the slow decay is originated from sample-to-sample fluctuations of the effective thresholds in finite-size networks can be put in a mathematical ground by approximating the sample average with an integral

$$\bar{\rho} = \int_0^\lambda d\lambda_c \rho(\lambda, \lambda_c) \mathcal{P}(\lambda_c) e^{-t/\tau(\lambda, \lambda_c)}. \quad (2)$$

Here $\rho(\lambda, \lambda_c)$ is the quasistatic density as a function of $\lambda > \lambda_c$ ($\rho \equiv 0$ for $\lambda < \lambda_c$), $\tau(\lambda, \lambda_c)$ is the lifetime of the dynamical processes and $\mathcal{P}(\lambda_c)$ is the probability density that a randomly selected sample has a threshold at λ_c .

We assume that in a free cutoff network with $\gamma > 2.5$ the activation happens at the most connected hub [41]. Consider a star subgraph, centered on the vertex of maximal degree k_{\max} , which forms an independently activated domain in a network with N nodes. Using QMF theory, the threshold in such a star graph is $\lambda_c \sim 1/\sqrt{k_{\max}}$ [28,46]. The density in a star of size k is $\rho_{\text{star}} \approx \lambda$ for $\lambda \gtrsim \lambda_c$, implying that

$$\rho = \frac{\lambda k_{\max}}{N}. \quad (3)$$

²The actual density in a star must increase a $\rho \sim \lambda^{\beta_{\text{star}}}$, where $\beta_{\text{star}} > \beta_{\text{QMF}} = 1$.

The lifespan of the activity in a star in case of SIS dynamics is [25]

$$\tau \simeq \tau_0 \exp(a\lambda^2 k_{\max}), \quad (4)$$

where a and τ_0 are constants. Finally, the probability of a given threshold is $\mathcal{P}(\lambda_c) d\lambda_c = \Pi(k_{\max}) dk_{\max}$, where

$$\Pi(k_{\max}) \simeq N \exp(-cNk_{\max}^{-\gamma+1}) k_{\max}^{-\gamma} \quad (5)$$

is the probability of the largest degree to be k_{\max} in a PL network with N vertices [27]. Here c is a constant depending on $P(k)$. Plugging Eqs. (3)–(5) into Eq. (2), we obtain

$$\bar{\rho} \sim \lambda \int_{1/\lambda^2}^{\infty} k_{\max}^{-\gamma+1} \exp(-cNk_{\max}^{-\gamma+1}) \exp(-t/\tau) dk_{\max}. \quad (6)$$

If $1/\lambda^2 \gg N^{1/(\gamma-1)}$, then the first exponential suppresses the integral and a standard subcritical phase with exponential decay is expected. For $1/\lambda^2 \lesssim N^{1/(\gamma-1)}$, the first exponential is approximately 1. After an integration by parts this integral can be easily evaluated using the saddle-point method to return $\bar{\rho} \sim (\ln t)^{-2-\gamma}$, exactly the result of Eq. (1). This decay is the same found by Lee *et al.* [30], in a theory of SIS dynamics for infinite PL networks, with noninteracting hubs. This predicts ultraslow decay instead of a stationary endemic state, contradicting the exact result of the null epidemic threshold for SIS irrespective of γ [23]. Why do our simulations match this theory? The assumption that stars form independent domains of activity is incorrect in principle, since the lifetime of epidemics on stars can be sufficiently large to permit mutual infection of hubs, even if they are not directly connected due to the small-world property [25,26]. However, several stars that contributed to the average epidemic activity in our simulations are observed in different realizations of networks and are thus actually independent.

In the SF regime at $\gamma = 2.7$ the QMF still predicts localization (see Appendix), but there is a high probability that several activated hubs occur in the same network sample even if their size is finite. Thus neglecting the multiplicity of activated hubs as well as the interaction among them [25] is not a quantitatively accurate approximation but it is able to capture the essentially logarithmically slow dynamics observed in simulations.

In case of hard cutoff, we do not know the form of $\mathcal{P}(\lambda_c)$. Since the fluctuations of λ_c depend on global properties of the networks, we assume their distribution to be Gaussian, with width $\sigma(N)$ and centered at $\lambda_0(N)$, tending to a delta function at $\lambda = 0$ as $N \rightarrow \infty$, in conformity with numerics. Less is known about the lifespan. Numerically, we have data consistent with $\tau \sim \exp[a(\lambda - \lambda_c)^2]$, where $a(N)$ is some function increasing with the size that we could not determine precisely. Plugging these forms into Eq. (2) and using the saddle-point approximation to solve the integral we found $\bar{\rho} \sim t^{-1/2a\sigma^2}$. This is a nonuniversal power law, in agreement with the density decay simulations, as far as $a\sigma^2$ is a nonuniversal constant.

V. QUASISTATIONARY ANALYSIS

The stationary state of the SIS model on a single finite network with degree exponent $\gamma > 3$ was characterized by multiple transitions as λ is varied due to the independent

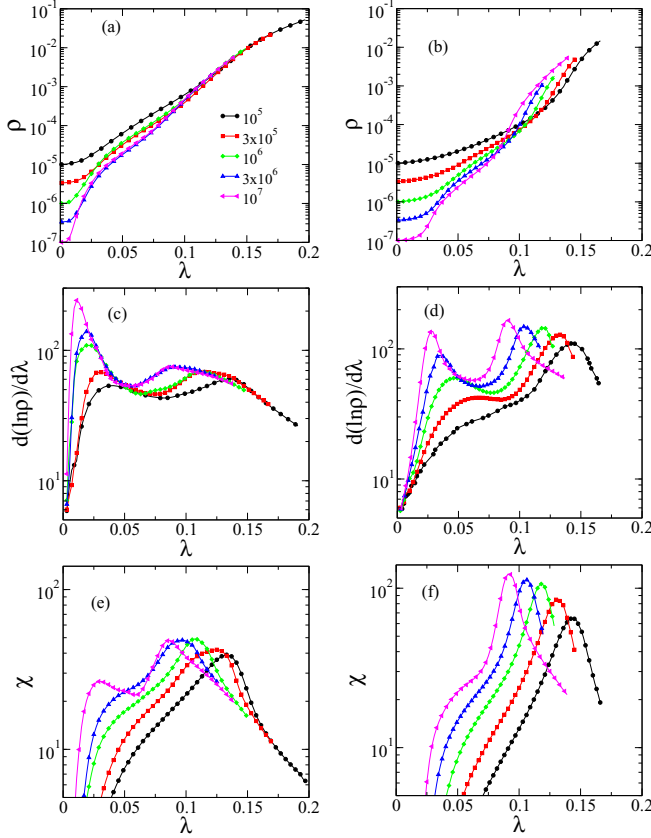


FIG. 6. Finite-size analysis of the QS state for networks with $\gamma = 3.5$. The [(a) and (b)] QS density ρ , [(c) and (d)] log-derivative of ρ , and [(e) and (f)] dynamical susceptibility are shown in left and right panels for free and hard cutoffs, respectively. The number of samples were at least $\mathcal{N} = 50$. The network sizes are indicated in the legend.

activation of different regions with different thresholds [31]. One transition was associated with the activation of the most connected vertex with a vanishing threshold of the QMF theory $\lambda_1 \sim 1/\sqrt{k_{\max}}$. A second transition was associated with the mutual activation of hubs [25] and took place at a threshold λ_2 . A third transition, that occurs at another finite threshold, was also found. This represents the collective activation of the network [26]. Again, we tackle this problem by averages over a large ensemble.

Figures 6(a) and 6(b) compares the QS density against λ for degree exponent $\gamma = 3.5$ with either hard or free cutoffs for networks of different sizes. The average QS density is a double sigmoid, a nonmonotonically increasing function of λ , which indicates two phase transitions. At a standard clean critical point, the logarithmic derivative of the QS density scales as [51]

$$\left. \frac{d \ln \rho}{d \lambda} \right|_{\lambda_c} \sim L^{1/\nu_{\perp}}, \quad (7)$$

where L is the system size and ν_{\perp} is a critical exponent associated with the divergence of the correlation length. This log-derivative can also be used to identify multiple transitions in epidemic spreading in networks [31], in association with the dynamical susceptibility $\chi = N(\langle \rho^2 \rangle - \langle \rho \rangle^2) / \langle \rho \rangle$ [28]. The

latter quantifies the relative fluctuations of the order parameter as shown in Fig. 6.

The log-derivative of the density is shown in Figs. 6(c) and 6(d), while the susceptibility is shown Figs. 6(e) and 6(f). Averages over the ensemble of networks wipe out the multiple transitions of single networks, leading to two observable transitions at thresholds λ_1 and $\lambda_2 > \lambda_1$. These correspond to the peaks of the log-derivatives and susceptibility; the latter is less evident for λ_1 . Notice that the double transition identified with the hard cutoff in the log-derivative analysis starts to emerge as a shoulder in the susceptibility curves of the largest size investigated. The threshold at λ_1 can clearly be seen in the susceptibility curves for natural cutoff only for very large sizes and is manifested as a shoulder for the other cases, including hard cutoffs.

For the free cutoff, a QS density $\rho_{\text{free}} \gg 1/N$, the minimal value allowed in a QS simulation, is observed in the interval $\lambda_1 < \lambda < \lambda_2$. This resembles a smeared phase transition [2] and the interval coincides with the region, where Griffiths effects are found in the density decay analysis. We attribute this smearing to the presence or absence of outliers in different samples. In the case of hard cutoff, the suppression of outliers leads to a weaker smearing with a density $1/N \ll \rho_{\text{hard}} \ll \rho_{\text{free}}$. In a standard smeared phase transition, patches having high-enough dimension can exhibit ordering transition independently. In principle outliers, represented by stars, are high-dimensional objects, which could be activated independently. So the basic ideas of smeared transitions could be fulfilled. However, outliers plus their neighbors provide a vanishing fraction of the network and give a vanishing contribution to the global density in the thermodynamic limit. Thus they generate a finite-size effect.

The finite-size analysis at thresholds $\lambda_{1,2}$ are shown in Fig. 7. The left threshold, determined via the log-derivative,

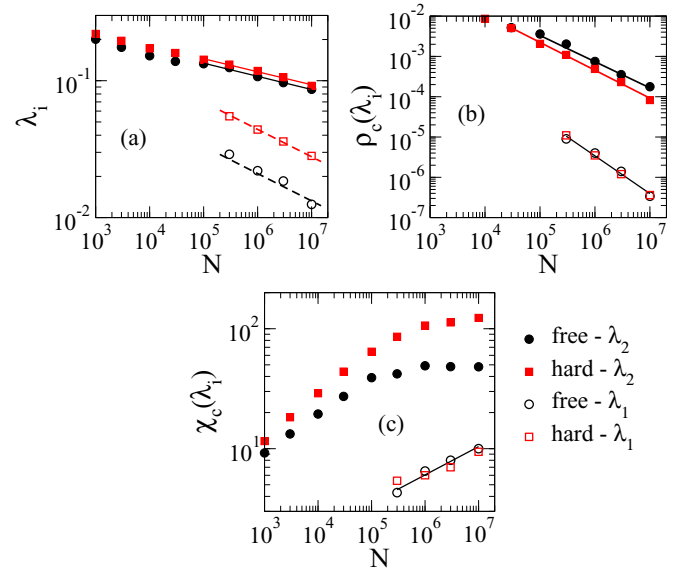


FIG. 7. Critical quantities against networks size for $\gamma = 3.5$: (a) threshold, (b) critical density, and (c) critical susceptibility at $\lambda = \lambda_i$. Solid lines are PL regressions while the dashed lines are $\lambda_1 \sim N^{-0.2}$ and $N^{-0.18}$ predicted by the QMF theory for free and hard cutoffs, respectively.

decays consistently with QMF theory and, for $\gamma > 2.5$, scales as $\lambda_1 \sim 1/\sqrt{k_{\max}} \sim N^{-0.5/(\gamma-1)}$ or $N^{-0.45/(\gamma-1)}$ for natural and hard cutoffs, respectively. This coincides with the activation of the star graph centered at the most connected vertex of the network [33]. The position of the right peak of the susceptibility, which agrees with the right one of log-derivative curves, goes slowly to zero as $\lambda_2(N) \sim N^{-0.09}$ in the investigated interval while the density evaluated at λ_2 follows a power law $\rho_c(\lambda_2) \sim N^{-0.65}$. These scaling laws are, within uncertainties, independent of the cutoff. However, both response functions, log-derivative and susceptibility, saturate with the size, confirming a smeared transition at λ_2 . The susceptibility at λ_1 , for free cutoff, increases as $\chi_c \sim N^{0.23}$, which is again consistent with the activation of the most connected vertex: For a star with k_{\max} leaves we have approximately $\chi \sim (k_{\max})^{0.55}$ (using data from Ref. [46]) and given that $k_{\max} \sim N^{1/(\gamma-1)}$, we obtain an exponent, which is close to 0.23, observed in the simulations.

The peaks at finite values of λ , observed in single networks [31], are wiped out and are not evident when averages are done.³

Analyzing the behavior for $N = 10^7$ with free cutoff and $\gamma = 3.5$, we found $\rho \sim \lambda^\beta$, where $\beta \approx 2.8$ with $\lambda_1 < \lambda < \lambda_2$. Running the dynamics only on the star centered on the most connected vertex by permanently immunizing the rest of the network, we found $\beta_{\text{star}} \approx 2.0 < \beta$. This means that the mutual activation of hubs is relevant in the interval $\lambda_1 < \lambda < \lambda_2$, leading to an exponent larger than that of a single star centered on the most connected vertex. The estimate $\beta \approx 2.8$ for $\gamma = 3.5$ is inside the rigorous bounds found by Chatterjee and Durrett [23]: $\gamma - 1 < \beta < 2\gamma - 3$.

VI. CONCLUSIONS

Random, scale-free networks exhibit strong, quenched inhomogeneities, and therefore rare region effects can be expected to play an important role. To see rare regions of arbitrary sizes we should simulate arbitrarily large system sizes or by the standard way of approximations we do sample averages over many independent network realizations. The latter way is not equivalent to the former one in scale-free networks. In models defined on networks with infinite topological dimensions, a recent hypothesis states that Griffiths phases cannot exist [3] and another important result for infinite dimensional networks with power-law degree distributions is that SIS does not exhibit a phase transition at finite λ [23]. Real networks, on the other hand, can be very large but are always finite. Therefore, a numerical analysis on different sizes is of great importance.

Here we present extensive simulations on networks generated with the configuration model using free (fluctuating) and structural or hard (nonfluctuating) degree cutoffs. We focused on statistics over a large ensemble of networks. Contrary

to the results obtained on single network realization, where multiple transitions were reported [31], we observe that the network ensemble averaging exhibits Griffiths effects in an extended region of the control parameter $\lambda_1(N) < \lambda < \lambda_2(N)$, which diminishes as network size increases and disappears in the thermodynamical limit. These Griffiths effects are due to sample-to-sample fluctuations, producing non-self-averaging within the shrinking critical dynamical region rather than the existence of RRs of actual Griffiths phases. We also observe the occurrence of a smeared transition, with saturated fluctuations of the order parameter at λ_2 . Our findings can be relevant if we consider independent realizations as graphs occurring in a sequence of uncorrelated, time-dependent networks at a given time and we measure quantities in the long-time average. Alternatively, such results can describe the behavior of systems in which power-law degree distribution in modules make up a very weakly coupled network.

More specifically for free cutoff networks, we found an asymptotic logarithmic decay of density in time in the interval $\lambda_1(N) < \lambda < \lambda_2(N)$. Here $\lambda_1 \sim 1/\sqrt{k_{\max}}$ is associated with the activation of the most connected vertex [33] and λ_2 describes the mutual activation of hubs that leads to an endemic phase of the network [25,26]. Both thresholds go to zero at the infinite size limit with $\lambda_2/\lambda_1 \rightarrow \infty$, implying that for finite sizes there exists a detectable extended interval with Griffiths effects. The logarithm decay is explained by an optimal fluctuation theory for networks where fluctuating pseudocritical points are considered. For structural and hard cutoffs the Griffiths effects are weaker, resulting in nonuniversal power-law density decay tails within a smaller range of the control parameter. We attribute this to the lack of outliers, which causes weaker sample-to-sample heterogeneity and less fluctuating pseudocritical points.

The finite-size analysis shows that the transition peaks move to zero by increasing the size and the Griffiths effects are replaced by a conventional critical point behavior characterized by $\beta \approx 2.8$ for degree exponent $\gamma = 3.5$.

ACKNOWLEDGMENTS

This work was supported by the funding agencies CNPq, CAPES, and FAPEMIG (Brazil) and the Hungarian research fund OTKA (Grant No. K109577). We thank Robert Juhász for fruitful comments and discussions. G.Ó. thanks the Physics Department at UFV, where part of this work was done, for its hospitality. S.C.F. thanks discussions with Romualdo Pastor-Satorras during visits to UFV supported by the program *Ciência sem Fronteiras*—CAPES (Grant No. 88881.030375/2013-01).

APPENDIX: SPECTRAL ANALYSIS FOR $\gamma = 2.7$

We have also tested whether the QMF theory provides localization for $2.5 < \gamma < 3$, since earlier numerical results suggested a localization transition at $\gamma = 3$ [34]. We performed spectral analysis of the SIS on UCM networks with $k_0 = 1, 2, 3$ structural and $k_0 = 2$ with free cutoff as described in Ref. [34] at $\gamma = 2.7$ for $N = 5000$ – 10^6 . We diagonalized the A_{ij} matrix which describes the evolution of activity

³In Ref. [31] networks with up to $N = 10^8$ vertices were simulated while here we analyzed until $N = 10^7$ and performed larger ensemble averaging. So our results do not definitely discard other transitions for higher sizes but no indications of them were observed in the investigated size range.

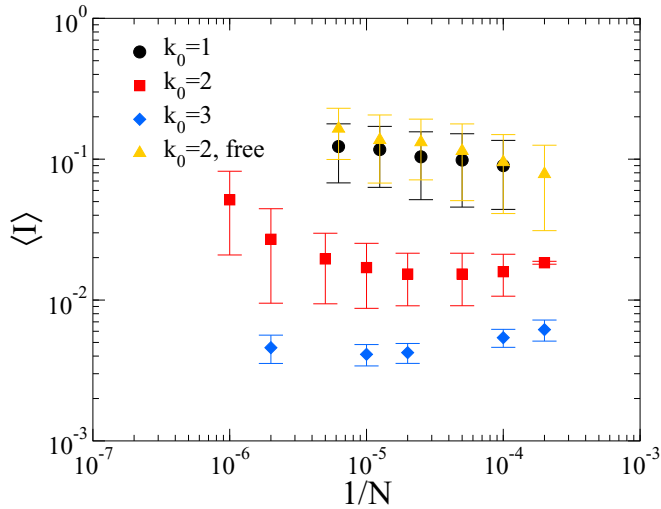


FIG. 8. Finite-size scaling of IPR for $\gamma = 2.7$, $k_0 = 1, 2, 3$, and structural and $k_0 = 2$ with free cutoff.

probabilities $\rho_i(t)$ of node i in the QMF approach

$$\frac{d\rho_i}{dt} = -\rho_i + \lambda(1 - \rho_i) \sum_{j=1}^N A_{ij} \rho_j. \quad (\text{A1})$$

The localization in the active steady state can be quantified by calculating the inverse participation ratio (IPR) of the principal eigenvector $e(y_1)$, related to the largest eigenvalue of the adjacency matrix as [29]

$$I(N) \equiv \sum_{i=1}^N e_i^4(y_1). \quad (\text{A2})$$

This quantity vanishes as $1/N$ in the case of homogeneous eigenvector components but remains finite as $N \rightarrow \infty$, if the activity is concentrated on a finite fraction of nodes. The average values $\langle I \rangle$ were determined for 100–1000 independent networks for each parameter value. The finite-size analysis (Fig. 8) for $k_0 = 1$ shows a clear monotonic increasing tendency of $\langle I \rangle$ as $N \rightarrow \infty$. In case of a $k_0 > 1$, the mean IPR values decrease first and cross over very slowly to an increase for $N > 10^5$. For free cutoff the graph generation is more difficult and slow, but, again, one can observe a monotonic increase of $\langle I \rangle$ up to $N = 160\,000$. Therefore, we see numerical evidence that epidemic activity of the QMF theory is localized at $\gamma = 2.7$ as expected, in general, for $\gamma > 2.5$ [29].

-
- [1] T. Vojta and M. Y. Lee, Nonequilibrium Phase Transition on a Randomly Diluted Lattice, *Phys. Rev. Lett.* **96**, 035701 (2006).
- [2] T. Vojta, Rare region effects at classical, quantum and nonequilibrium phase transitions, *J. Phys. A: Math. Gen.* **39**, R143 (2006).
- [3] M. A. Muñoz, R. Juhász, C. Castellano, and G. Ódor, Griffiths Phases on Complex Networks, *Phys. Rev. Lett.* **105**, 128701 (2010).
- [4] P. Moretti and M. A. Muñoz, Griffiths phases and the stretching of criticality in brain networks, *Nat. Commun.* **4**, 2521 (2013).
- [5] A. J. Noest, New Universality for Spatially Disordered Cellular Automata and Directed Percolation, *Phys. Rev. Lett.* **57**, 90 (1986).
- [6] M. Bramson, R. Durrett, and R. H. Schonmann, The contact processes in a random environment, *Ann. Probab.* **19**, 960 (1991).
- [7] A. G. Moreira and R. Dickman, Critical dynamics of the contact process with quenched disorder, *Phys. Rev. E* **54**, R3090 (1996).
- [8] M. M. de Oliveira and S. C. Ferreira, Universality of the contact process with random dilution, *J. Stat. Mech.: Theor. Exp.* (2008) P11001.
- [9] T. Vojta, A. Farquhar, and J. Mast, Infinite-randomness critical point in the two-dimensional disordered contact process, *Phys. Rev. E* **79**, 011111 (2009).
- [10] H. Barghathi and T. Vojta, Phase Transitions on Random Lattices: How Random is Topological Disorder? *Phys. Rev. Lett.* **113**, 120602 (2014).
- [11] J. Hooyberghs, F. Iglói, and C. Vanderzande, Absorbing state phase transitions with quenched disorder, *Phys. Rev. E* **69**, 066140 (2004).
- [12] M. M. de Oliveira, S. G. Alves, S. C. Ferreira, and R. Dickman, Contact process on a Voronoi triangulation, *Phys. Rev. E* **78**, 031133 (2008).
- [13] R. Juhász, G. Ódor, C. Castellano, and M. A. Muñoz, Rare-region effects in the contact process on networks, *Phys. Rev. E* **85**, 066125 (2012).
- [14] G. Ódor, R. Dickman, and G. Ódor, Griffiths phases and localization in hierarchical modular networks, *Sci. Rep.* **5**, 14451 (2015).
- [15] P. Bak, C. Tang, and K. Wiesenfeld, Self-Organized Criticality: An Explanation of the $1/f$ Noise, *Phys. Rev. Lett.* **59**, 381 (1987).
- [16] Robert B. Griffiths, Nonanalytic Behavior Above the Critical Point in a Random Ising Ferromagnet, *Phys. Rev. Lett.* **23**, 17 (1969).
- [17] A. Barrat, M. Barthélemy, and A. Vespignani, *Dynamical Processes on Complex Networks* (Cambridge University Press, Cambridge, New York, 2008).
- [18] S. N. Dorogovtsev, A. V. Goltsev, and J. F. F. Mendes, Critical phenomena in complex networks, *Rev. Mod. Phys.* **80**, 1275 (2008).
- [19] M. E. J. Newman, *Networks: An Introduction* (Oxford University Press, Oxford, 2010).
- [20] R. Albert and A.-L. Barabási, Statistical mechanics of complex networks, *Rev. Mod. Phys.* **74**, 47 (2002).
- [21] T. E. Harris, Contact interactions on a lattice, *Ann. Probab.* **2**, 969 (1974).
- [22] R. Pastor-Satorras and A. Vespignani, Epidemic Spreading in Scale-Free Networks, *Phys. Rev. Lett.* **86**, 3200 (2001).
- [23] S. Chatterjee and R. Durrett, Contact processes on random graphs with power law degree distributions have critical value 0, *Ann. Probab.* **37**, 2332 (2009).

- [24] T. Mountford, J.-C. Mourrat, D. Valesin, and Q. Yao, Exponential extinction time of the contact process on finite graphs, [arXiv:1203.2972v1](#) [Stochastic Processes and their Applications (to be published)].
- [25] M. Boguñá, C. Castellano, and R. Pastor-Satorras, Nature of the Epidemic Threshold for the Susceptible-Infected-Susceptible Dynamics in Networks, *Phys. Rev. Lett.* **111**, 068701 (2013).
- [26] S. C. Ferreira, R. S. Sander, and R. Pastor-Satorras, Collective versus hub activation of epidemic phases on networks, *Phys. Rev. E* **93**, 032314 (2016).
- [27] M. Boguñá, R. Pastor-Satorras, and A. Vespignani, Cut-offs and finite size effects in scale-free networks, *Eur. Phys. J. B* **38**, 205 (2004).
- [28] S. C. Ferreira, C. Castellano, and R. Pastor-Satorras, Epidemic thresholds of the susceptible-infected-susceptible model on networks: A comparison of numerical and theoretical results, *Phys. Rev. E* **86**, 041125 (2012).
- [29] A. V. Goltsev, S. N. Dorogovtsev, J. G. Oliveira, and J. F. F. Mendes, Localization and Spreading of Diseases in Complex Networks, *Phys. Rev. Lett.* **109**, 128702 (2012).
- [30] H. K. Lee, P.-S. Shim, and J. D. Noh, Epidemic threshold of the susceptible-infected-susceptible model on complex networks, *Phys. Rev. E* **87**, 062812 (2013).
- [31] A. S. Mata and S. C. Ferreira, Multiple transitions of the susceptible-infected-susceptible epidemic model on complex networks, *Phys. Rev. E* **91**, 012816 (2015).
- [32] Y. Wang, D. Chakrabarti, C. Wang, and C. Faloutsos, Epidemic spreading in real networks: An eigenvalue viewpoint, in *22nd International Symposium on Reliable Distributed Systems (SRDS'03)* (IEEE Computer Society, Los Alamitos, CA, 2003), pp. 25–34.
- [33] C. Castellano and R. Pastor-Satorras, Thresholds for Epidemic Spreading in Networks, *Phys. Rev. Lett.* **105**, 218701 (2010).
- [34] G. Ódor, Localization transition, Lifschitz tails, and rare-region effects in network models, *Phys. Rev. E* **90**, 032110 (2014).
- [35] G. Ódor and R. Pastor-Satorras, Slow dynamics and rare-region effects in the contact process on weighted tree networks, *Phys. Rev. E* **86**, 026117 (2012).
- [36] G. Ódor, Rare regions of the susceptible-infected-susceptible model on Barabási-Albert networks, *Phys. Rev. E* **87**, 042132 (2013).
- [37] G. Ódor, Spectral analysis and slow spreading dynamics on complex networks, *Phys. Rev. E* **88**, 032109 (2013).
- [38] C. Buono, F. Vazquez, P. A. Macri, and L. A. Braunstein, Slow epidemic extinction in populations with heterogeneous infection rates, *Phys. Rev. E* **88**, 022813 (2013).
- [39] L. K. Gallos, H. Makse, and M. Sigman, A small world of weak ties provides optimal global integration of self-similar modules in functional brain networks, *Proc. Natl. Acad. Sci. USA* **109**, 2825 (2012).
- [40] P. Villegas, P. Moretti, and M. A. Munoz, Frustrated hierarchical synchronization and emergent complexity in the human connectome network, *Sci. Rep.* **4**, 5990 (2014).
- [41] C. Castellano and R. Pastor-Satorras, Competing activation mechanisms in epidemics on networks, *Sci. Rep.* **2**, 371 (2012).
- [42] J. Marro and R. Dickman, *Nonequilibrium Phase Transitions in Lattice Models* (Cambridge University Press, Cambridge, 1999).
- [43] M. M. de Oliveira and R. Dickman, How to simulate the quasistationary state, *Phys. Rev. E* **71**, 016129 (2005).
- [44] R. Pastor-Satorras and C. Castellano, Distinct types of eigenvector localization in networks, *Sci. Rep.* **6**, 18847 (2016).
- [45] M. Catanzaro, M. Boguñá, and R. Pastor-Satorras, Generation of uncorrelated random scale-free networks, *Phys. Rev. E* **71**, 027103 (2005).
- [46] A. S. Mata and S. C. Ferreira, Pair quenched mean-field theory for the susceptible-infected-susceptible model on complex networks, *Europhys. Lett.* **103**, 48003 (2013).
- [47] A. Aharony and A. B. Harris, Absence of Self-Averaging and Universal Fluctuations in Random Systems Near Critical Points, *Phys. Rev. Lett.* **77**, 3700 (1996).
- [48] R. Pastor-Satorras, A. Vázquez, and A. Vespignani, Dynamical and Correlation Properties of the Internet, *Phys. Rev. Lett.* **87**, 258701 (2001).
- [49] S. C. Ferreira, R. S. Ferreira, C. Castellano, and R. Pastor-Satorras, Quasistationary simulations of the contact process on quenched networks, *Phys. Rev. E* **84**, 066102 (2011).
- [50] A. S. Mata, R. S. Ferreira, and S. C. Ferreira, Heterogeneous pair-approximation for the contact process on complex networks, *New J. Phys.* **16**, 053006 (2014).
- [51] R. Dickman, Critical exponents for the restricted sandpile, *Phys. Rev. E* **73**, 036131 (2006).